Available online at www.sciencedirect.com
SCIENCE DIRECT®
Journal of Photochemistry and Photobiology A: Chemistry 168 (2004) 47–52
Journal of Photochemistry and Photobiology A:Chemistry
www.elsevier.com/locate/jphotochem

Enhanced photocatalytic performance of nanosized coupled ZnO/SnO_2 photocatalysts for methyl orange degradation

Cun Wang [a,b], Xinming Wang [b], Bo-Qing Xu [a,*], Jincai Zhao [c], Bixian Mai [b], Ping'an Peng [b], Guoying Sheng [b], Jiamo Fu [b]

[a] *Department of Chemistry, Tsinghua University, Beijing 100084, China*
[b] *Guangzhou Institute of Geochemistry, Chinese Academy of Sciences, Guangzhou 510640, China*
[c] *Institute of Chemistry, Chinese Academy of Sciences, Beijing 100080, China*

Received 4 November 2003; received in revised form 15 April 2004; accepted 18 May 2004
Available online 2 July 2004

Abstract

Nanosized coupled ZnO/SnO_2 photocatalysts with different Sn contents were prepared using the coprecipitation method, and characterized by X-ray diffraction, specific surface area and UV-Vis diffuse reflectance spectroscopy. The phases, mean grain sizes and band gap energy of the coupled ZnO/SnO_2 photocatalysts varied with the Sn contents and the calcination temperatures. The photocatalytic activities of the coupled ZnO/SnO_2 photocatalysts, evaluated using the photodegradation of methyl orange as a probe reaction, were also found to be related to the calcination temperatures and the Sn contents. The photocatalytic activities of the coupled ZnO/SnO_2 photocatalysts decreased with the increasing calcination temperatures. The maximum photocatalytic activity of the coupled ZnO/SnO_2 photocatalyst, which is about 1.3 times the photocatalytic activity of ZnO and 21.3 times that of SnO_2, was observed with a Sn content of 33.3 mol% under calcination at 500 °C for 10 h. The enhancement of the photocatalytic activity might arise from the hetero-junctions ZnO/SnO_2 in the coupled oxides. The photo-stability of the ZnO/SnO_2 photocatalyst was also studied.
© 2004 Elsevier B.V. All rights reserved.

Keywords: Photocatalysis; Zinc oxide; Tin dioxide; Nanomaterials; Methyl orange

1. Introduction

Photocatalytic degradation of organic pollutants in water and air using semiconductors, such as TiO_2 and ZnO, has attracted extensive attention in the past two decades [1]. Previous studies have proved that such semiconductors can degrade most kinds of persistent organic pollutants, such as detergents, dyes, pesticides and volatile organic compounds, under UV-irradiation. However, the fast recombination rate of the photogenerated electron/hole pairs hinders the commercialization of this technology [1]. It is of great interest to improve the photocatalytic activity of semiconductors for the degradation of organic compounds in water and air. In the past decade years, there are a number of studies related to the photocatalytic activity of TiO_2 or ZnO coupled with metal oxides, like SnO_2 [2,3], WO_3 [4], Fe_2O_3 [5], ZrO_2 [6] and some rare earth oxides [7], for the purpose of improving the photocatalytic activity of TiO_2 or ZnO. Coupled semiconductor photocatalysts may increase the photocatalytic efficiency by increasing the charge separation and extending the photo-responding range. At the same time, their physical and optical properties are greatly modified [4].

The aim of this study is to optimize the preparation for the coupled ZnO/SnO_2 photocatalysts. For that purpose, a series of nanosized coupled ZnO/SnO_2 photocatalysts with different Sn contents were prepared and their photocatalytic activities were evaluated using methyl orange as a model organic compound. Furthermore, the diffuse reflectance spectra of the coupled ZnO/SnO_2 photocatalysts were measured, and their band gap energies were calculated according to the spectra. The effect of the heat-treating condition on the photocatalytic activities of the coupled ZnO/SnO_2 photocatalysts has been studied. The photo-stability of

* Corresponding author. Tel.: +86-10-62772592; fax: +86-10-62792122.
E-mail address: bqxu@mail.tsinghua.edu.cn (B.-Q. Xu).

1010-6030/$ – see front matter © 2004 Elsevier B.V. All rights reserved.
doi:10.1016/j.jphotochem.2004.05.014

the coupled ZnO/SnO_2 photocatalyst with a Sn content of 33.3 mol% has also been examined.

2. Experimental

2.1. Preparation of nanosized photocatalysts

The nanosized coupled ZnO/SnO_2 photocatalysts were prepared using the coprecipitation method. $SnCl_4{\cdot}5H_2O$ and $ZnSO_4{\cdot}7H_2O$ (Analytic reagent grade, or A.R.) were used as the starting materials, and NaOH (A.R.) was used as the coprecipitant without further purification. $ZnSO_4{\cdot}7H_2O$ and $SnCl_4{\cdot}5H_2O$ in the molar ratios of 20:1, 2:1, 1:1, 1:2 and 1:20 were dissolved in a minimum amount of deionized water for the preparation of the coupled ZnO/SnO_2 photocatalysts with the Zn/Sn molar ratios of 20:1, 2:1, 1:1, 1:2 and 1:20, labeled by $Z_{20}S_1$, Z_2S_1, Z_1S_1, Z_1S_2 and Z_1S_{20}, respectively. Then the 4 mol l^{-1} NaOH solution was added, respectively, into the above solutions to adjust the pH to about 7, and the white amorphous precipitates were formed. The precipitates were filtered and washed with deionized water until no SO_4^{2-} and Cl^- were found in the filtrates. Then the wet powders were dried at about 100 °C in air to form the precursors of the coupled ZnO/SnO_2 photocatalysts. Finally the precursors were calcined in air to prepare the nanosized photocatalysts. The nanosized ZnO (Z) and SnO_2 (S) were prepared using the same procedure as mentioned above except that the starting materials are $ZnSO_4{\cdot}7H_2O$ for ZnO and $SnCl_4{\cdot}5H_2O$ for SnO_2, respectively.

2.2. Characterization of photocatalysts

To determine the crystal phase composition of the coupled ZnO/SnO_2 photocatalyst powders, X-ray powder diffraction (XRD) analysis was carried out at room temperature using a Rigaku D/max-1200 diffractometer with Cu Kα radiation ($\lambda = 0.15418$ nm), over the 2θ collection range of 10–60°. The accelerating voltage of 40 kV, emission current of 30 mA and the scanning speed of 4° min^{-1} were used. UV-Vis diffuse reflectance spectra (UV-Vis DRS) were recorded in air at room temperature in the wavelength range of 200–700 nm using a Hitachi U-3010 spectrophotometer with an integrating sphere. The pure powdered $BaSO_4$ was used as a reference sample. Specific surface areas (S_{BET}) were measured with Brunauer–Emmett–Teller (BET) method using a Quantachrome NOVA/1000 gas (N_2) analyzer.

2.3. Photocatalytic activity measurements

The photodegradation of methyl orange (MO) in aqueous solution was monitored in the presence of various coupled ZnO/SnO_2 photocatalyst powders. The MO is A.R. grade and was used as supplied. The photocatalytic reactor consists of two parts: a 100 ml Pyrex glass bottle and a 300 W high pressure Hg lamp with a maximum emission at about 365 nm, which was positioned parallel to the Pyrex glass bottle. In all experiments, the photocatalytic reaction temperature was kept at about 35 °C.

Reaction suspensions were prepared by adding photocatalyst powders into 100 ml MO solutions. The suspensions were ultrasonically sonicated for 15 min and then magnetically stirred in dark for 30 min to ensure an adsorption/desorption equilibrium prior to the UV-irradiation. The suspensions containing MO and photocatalysts were then irradiated by the UV light with continuous stirring.

Analytical samples were drawn from the reaction suspensions after various reaction times and centrifuged at 9000 rpm for 10 min, and then filtered through a 0.2 μm millipore filter to remove the particles. The MO concentrations of the filtrates were analyzed by UV-Vis spectroscopy (Thermo Spectronic/Heλios α) at its maximum absorption wavelength of 464 nm. Total organic carbon (TOC) measurements of the filtrates were conducted using a Dohrmann/Phoenix 8000/UV-Persulfate TOC analyzer.

3. Results and discussion

3.1. Phase and main grain size of photocatalysts

The precursors of the coupled ZnO/SnO_2 photocatalysts were calcined at 500, 700 and 900 °C for 10 h to prepare the photocatalysts. For brevity, only the XRD patterns of the coupled ZnO/SnO_2 photocatalyst powders with different Sn contents calcined at 700 °C for 10 h are shown in Fig. 1.

The phases and the mean grain sizes of the coupled ZnO/SnO_2 photocatalysts were determined according to the XRD results (Table 1). The mean grain sizes were estimated by using the Scherrer formula [8] and selecting the crystal planes of (1 0 1), (1 1 0) and (3 1 1) for ZnO, SnO_2 and Zn_2SnO_4, respectively.

It can be seen from Table 1 that for the pure SnO_2 (cassiterite) and ZnO (zincite) samples, no changes in the phases were observed, but the mean grain sizes of the SnO_2 and the ZnO became larger with the increasing calcination tem-

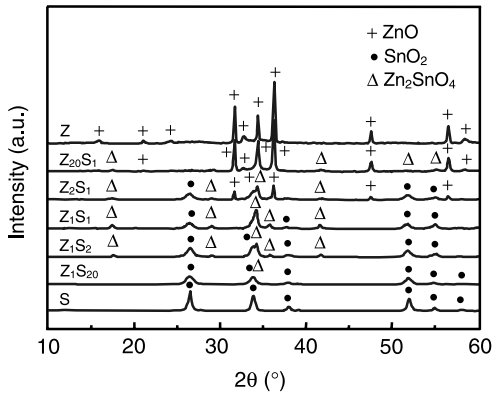

Fig. 1. XRD patterns of the coupled ZnO/SnO_2 photocatalyst powders calcined at 700 °C for 10 h.

Table 1
Relationship of phase, mean grain size, composition and calcination temperature

Sample	Sn content[a] (mol%)	Phase/mean grain size (nm)		
		500 °C[b,c]	700 °C[b,c]	900 °C[b,c]
Z	0	ZnO/60.3	ZnO/115.8	ZnO/215.2
$Z_{20}S_1$	4.8	ZnO/51.9 SnO_2/n.d.[d] –	ZnO/88.6 – Zn_2SnO_4/a few	ZnO/100.4 – Zn_2SnO_4/a few
Z_2S_1	33.3	ZnO/48.6 SnO_2/2.0 –	ZnO/79.3 SnO_2/10.8 Zn_2SnO_4/71.3	ZnO/a few SnO_2/a few Zn_2SnO_4/115.2
Z_1S_1	50	ZnO/8.5 SnO_2/2.7 –	– SnO_2/11.0 Zn_2SnO_4/36.5	– SnO_2/77.4 Zn_2SnO_4/99.8
Z_1S_2	66.7	ZnO/3.1 SnO_2/3.6 –	– SnO_2/14.6 Zn_2SnO_4/28.3	– SnO_2/58.5 Zn_2SnO_4/88.1
Z_1S_{20}	95.2	ZnO/n.d. SnO_2/6.9 –	– SnO_2/17.2 Zn_2SnO_4/a few	– SnO_2/50.7 Zn_2SnO_4/a few
S	100	SnO_2/11.4	SnO_2/25.8	SnO_2/44.6

[a] Molar fraction of Sn in total Zn and Sn (the same hereinafter).
[b] Calcination temperature.
[c] All samples were calcined for 10 h.
[d] Could not be detected.

perature. For all the coupled ZnO/SnO_2 photocatalysts, a solid reaction between the ZnO and SnO_2 to form an inverse spinel-type Zn_2SnO_4 phase (JCPDS 74-2184) took place at 700 °C and continued at 900 °C. The reaction between ZnO and SnO_2 to form Zn_2SnO_4 is expressed as follows [9]:

$$2ZnO + SnO_2 \rightarrow Zn_2SnO_4$$

Therefore, the formation temperature of Zn_2SnO_4 with the coprecipitation method is about 700 °C, which is about 300 °C lower than that (about 1000 °C) with the solid reaction method [9,10]. For Z_1S_1, Z_1S_2 and Z_1S_{20}, the phase compositions were the mixture of ZnO and SnO_2 when calcining at 500 °C for 10 h (ZnO for Z_1S_{20} was not detected by XRD due to its low content), but became the mixture of SnO_2 and Zn_2SnO_4 because all the ZnO had reacted with SnO_2 when calcining at 700 and 900 °C for 10 h. For Z_2S_1, when calcining at 500 °C for 10 h the phase compositions were also the mixture of SnO_2 and ZnO, but when calcining at 700 and 900 °C for 10 h the phase compositions were the mixture of ZnO, SnO_2 and Zn_2SnO_4, and only a few ZnO and SnO_2 remained after calcination for 10 h at 900 °C. It can be estimated approximately from the XRD intensities that about 60 and 95 mol% of total ZnO had reacted with SnO_2 to form Zn_2SnO_4 after the Z_2S_1 was calcined at 700 and 900 °C for 10 h. For $Z_{20}S_1$, when calcining at 500 °C for 10 h, only ZnO could be observed. SnO_2 was not detected because of its very low content. After calcining at 700 and 900 °C for 10 h, the powders were the mixture of ZnO and Zn_2SnO_4, since all the SnO_2 had reacted with ZnO to form Zn_2SnO_4.

It can be seen from Table 1 that the mean grain size of the ZnO in the pure ZnO sample was always much larger than that of the SnO_2 in the pure SnO_2 sample under the same calcination conditions. This is another fact that ZnO sinters more easily, and therefore it tends to have larger grain size than SnO_2 [11]. For the coupled ZnO/SnO_2 photocatalysts, not only the growth of the ZnO grain was inhibited by the SnO_2 coexisted, but also the inhibitive effect enhanced as the SnO_2 content increased. This is in agreement with the literature results that the addition of SnO_2 into ZnO causes a decrease in the mean grain size of ZnO [12,13]. Table 1 also indicates that when calcining at 500 and 700 °C, the growth of the SnO_2 grain was also inhibited by the ZnO coexisted, and the inhibitive effect enhanced as the ZnO content increased. This is similar to the case of ZnO and agrees with the literature result [14]. A possible explanation is that both the sintering between particles and the growth of the SnO_2 grain proceeded through a surface diffusion mechanism, and the ZnO particles could disperse on the SnO_2 surface [14], leading the growth of the SnO_2 grain to be inhibited by the ZnO. By contrast, when calcining at 900 °C, the ZnO coexisted seemed to favor the growth of the SnO_2 grain. This may be due to that the Zn_2SnO_4 formed promoted the growth of the SnO_2 grain under such high calcination temperature as 900 °C.

3.2. UV-Vis DRS and band gap energy

The room temperature UV-Vis diffuse reflectance spectra of the S, Z_1S_{20}, Z_1S_2, Z_1S_1, Z_2S_1, $Z_{20}S_1$ and Z powders calcined at 500, 700 and 900 °C for 10 h were displayed in Fig. 2. The wavelengths of absorption edges were determined by extrapolating the horizontal and sharply rising portions of the curve and defining the edge as the wavelength of the intersection [15]. The absorption edges thus determined are given in Table 2. The band gap energies (E_g) calculated on the basis of the corresponding absorption edges are shown in Fig. 3 [16]. As shown in Table 1, the coupled ZnO/SnO_2 photocatalysts calcined at 500, 700 and 900 °C for 10 h are the mixtures of ZnO, SnO_2 and/or Zn_2SnO_4, so the band gap energies of the coupled ZnO/SnO_2 pho-

Table 2
Relationship of composition, calcination temperature and absorption edge

Sample	Sn content (mol%)	Absorption edge (nm)		
		500 °C[a,b]	700 °C[a,b]	900 °C[a,b]
Z	0	388.9	386.9	390.6
$Z_{20}S_1$	4.8	391.2	387.5	386.3
Z_2S_1	33.3	397.5	388.7	361.1
Z_1S_1	50	402.8	389.9	353.4
Z_1S_2	66.7	415.6	397.2	358.9
Z_1S_{20}	95.2	466.1	434.2	373.3
S	100	485.3	482.5	463.1

[a] Calcination temperature.
[b] All samples were calcined for 10 h.

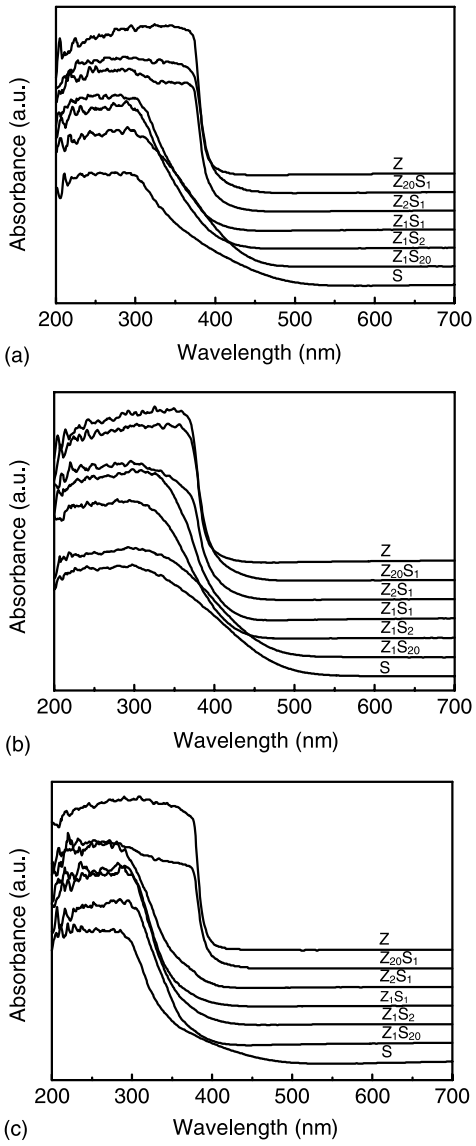

Fig. 2. UV-Vis diffuse reflectance absorption spectra of the coupled ZnO/SnO_2 photocatalyst powders calcined at (a) 500, (b) 700 and (c) 900 °C for 10 h.

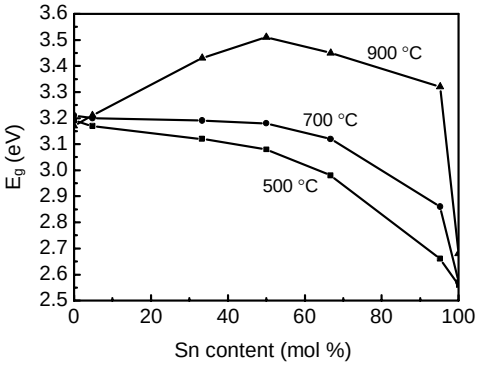

Fig. 3. Effect of the Sn content on the band gap energy of the coupled ZnO/SnO_2 photocatalysts calcined at 500, 700 and 900 °C for 10 h.

tocatalysts should originate from the overlapping of the corresponding ZnO, SnO_2 and/or Zn_2SnO_4 components in the coupled oxides. It can be seen from Table 2 and Fig. 3 that the absorption edge of the coupled ZnO/SnO_2 photocatalyst, or the band gap energy, changed with the Sn content and the calcination temperature. When calcining at 500 and 700 °C, the band gap energy of the coupled ZnO/SnO_2 photocatalyst decreased with the increasing SnO_2 content. When calcining at 900 °C, however, the band gap energy increased to a maximum at the Sn content of 50 mol% and then decreased as the Sn content further increased. For the coupled ZnO/SnO_2 photocatalyst with a fixed Sn content, the band gap energy increased with the calcination temperature. These changes in band gap energy may be due to the change in the ratio of the ZnO, SnO_2 and/or Zn_2SnO_4 in the coupled ZnO/SnO_2 photocatalysts, which is controlled by the Sn content and the calcination conditions. The band gap energies of ZnO, SnO_2 and Zn_2SnO_4 were reported to be 3.2 eV [16], 3.2 eV [16] and 3.4 eV [17], respectively. The band gap energies of the pure ZnO samples calcined at 500, 700 and 900 °C for 10 h were measured to be 3.19, 3.20 and 3.17 eV, respectively, which are in reasonable agreement with the accepted literature value of 3.2 eV [16] taking into account the experimental errors, indicating that the band gap energy of the ZnO has no relation with the calcination temperature. It can also be seen from Fig. 2 that the absorption curves of the SnO_2 samples calcined at 500, 700 and 900 °C for 10 h, and those of the Z_1S_{20} samples calcined at 500 and 700 °C for 10 h, displayed significant energy tail. But the energy tail of the Z_1S_{20} disappeared when the calcination temperature was increased to 900 °C. This indicates that the SnO_2 samples calcined at 500, 700 and 900 °C and the Z_1S_{20} samples calcined at 500 and 700 °C, showed indirect transition, whereas the Z_1S_{20} sample calcined at 900 °C only showed direct transition [18–20]. It was reported that SnO_2 is an n-type semiconductor oxide not only with the direct band gap energy of 3.5–3.9 eV [18–22] but also with the indirect band gap energy of around 2.6 eV [18–20]. The indirect band gap energies of the SnO_2 samples calcined at 500, 700 and 900 °C for 10 h were measured to be 2.56, 2.57 and 2.68 eV, respectively, indicating that the indirect band gap energy of the SnO_2 increased with the increasing calcination temperature. It should be noted that the above three indirect band gap energies of the SnO_2 are reasonable, because the colors (light-yellow) of the SnO_2 samples were consistent with the corresponding optical spectra [23].

3.3. Photocatalytic activity

The structural formula of methyl orange is shown in Scheme 1.

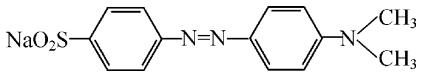

Scheme 1.

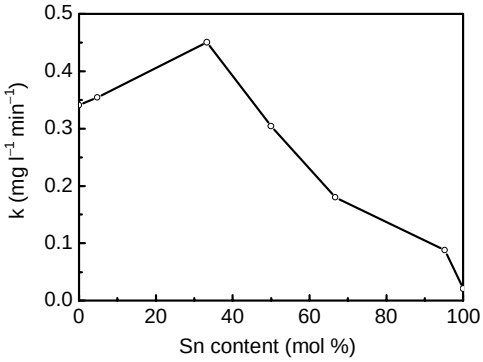

Fig. 4. The photocatalytic activity as a function of the Sn content for the coupled ZnO/SnO_2 photocatalysts calcined at 500 °C for 10 h (photocatalytic reaction rate constants (k) were calculated considering the initial 20 min of irradiation, i.e. $k = (C_0 - C_{20})/20$, where C_0 and C_{20} are the equilibrium concentrations of MO before and after 20 min UV-irradiation, respectively). Photocatalysts: 2.5 g l^{-1}; MO: 20 mg l^{-1}.

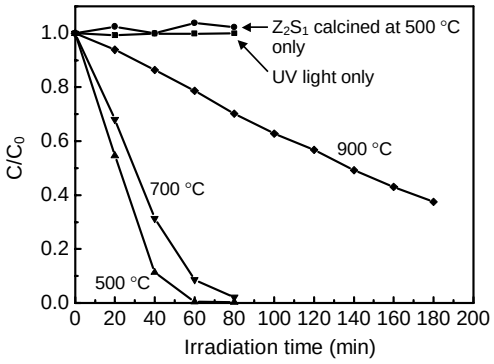

Fig. 5. Degradation kinetics of MO over the Z_2S_1 photocatalysts calcined at 500, 700 and 900 °C for 10 h (C_0 and C are the equilibrium concentrations of MO before and after UV-irradiation, respectively). Z_2S_1: 2.5 g l^{-1}; MO: 20 mg l^{-1}.

The photocatalytic activities of the coupled ZnO/SnO_2 photocatalysts with different Sn contents calcined at 500 °C for 10 h is shown in Fig. 4. It can be seen from Fig. 4 that pure SnO_2 showed very low photocatalytic activity and pure ZnO showed higher photocatalytic activity, which agrees with the previous report [1,16]. Therefore, the Sn content should be an important factor affecting the photocatalytic activity of the coupled ZnO/SnO_2 photocatalyst. It can be seen that the $Z_{20}S_1$ and Z_2S_1 photocatalysts displayed higher photocatalytic activity than pure ZnO and SnO_2, and the photocatalytic activity of the coupled ZnO/SnO_2 photocatalyst changed with the Sn content. The optimum Sn content was found at 33.3 mol%, at which the photocatalytic activity of the coupled ZnO/SnO_2 photocatalyst is about 1.3 times that of the ZnO and 21.3 times that of the SnO_2. The enhancement in the photocatalytic activity may come from the hetero-junctions ZnO/SnO_2 in the coupled ZnO/SnO_2 photocatalysts [2]. For the coupled ZnO/SnO_2 photocatalyst calcined at 500 °C for 10 h, as the Sn content increased up to 33.3 mol%, the photocatalytic activity should increase gradually due to that the number of the hetero-junctions ZnO/SnO_2 increased [2,24]. But further increasing the SnO_2 content led to a decrease in the photocatalytic activity of the coupled ZnO/SnO_2 photocatalyst because of the very low photocatalytic activity of SnO_2. The specific surface areas of the Z, $Z_{20}S_1$, Z_2S_1, Z_1S_1, Z_1S_2, Z_1S_{20} and S powders calcined at 500 °C for 10 h were measured to be 6.4, 17.6, 36.1, 38.2, 48.2, 43.6 and 35.2 m^2 g^{-1}, respectively, indicating that the specific surface area increased as the Sn content was increased up to 66.7 mol%, which led the photocatalytic activity to increase accordingly. Therefore, for the coupled ZnO/SnO_2 photocatalysts, the maximum photocatalytic activity appeared at the Sn content of 33.3 mol% due to the above conflicting factors that affect the overall photocatalytic activity.

Fig. 5 shows the degradation kinetics of MO over the Z_2S_1 photocatalysts calcined at 500, 700 and 900 °C for 10 h. A blank experiment in the absence of the UV-irradiation but with the Z_2S_1 calcined at 500 °C for 10 h demonstrated that no MO degradation occurred. Another blank experiment in the absence of the photocatalyst but under the UV-irradiation showed that MO could not be degraded. The results of the blank experiments are as shown in Fig. 5. It can be seen from Fig. 5 that the photocatalytic activity of the Z_2S_1 decreased slightly when the calcination temperature was increased from 500 to 700 °C, but decreased significantly when the calcination temperature was increased to 900 °C. A main reason may be that the residual ZnO decreased significantly as the calcination temperature was increased: about 40 mol% of total ZnO still remained after calcination for 10 h at 700 °C, but only about 5 mol% of total ZnO remained after calcination for 10 h at 900 °C because about 95 mol% of total ZnO had reacted with the SnO_2 to form Zn_2SnO_4 with a little photocatalytic activity [25,26]. The photocatalytic activity of the Z_2S_1 calcined at 900 °C for 10 h may mostly arise from the residual ZnO (about 5 mol% of total ZnO). The specific surface areas of the Z_2S_1 photocatalysts calcined at 500, 700 and 900 °C for 10 h were measured to be 36.1, 20.5 and 2.2 m^2 g^{-1}, respectively. Therefore, the specific surface area of the Z_2S_1 photocatalyst decreased significantly with the increasing calcination temperature, thus led to decrease in photocatalytic activity. It can be seen from Fig. 5 that the MO solution can be decolorized completely over the Z_2S_1 calcined at 500 °C for 10 h after about 60 min UV-irradiation, indicating that the Z_2S_1 shows higher photocatalytic activity to methyl orange.

Fig. 6 shows the TOC elimination kinetics of MO over the Z_2S_1 calcined at 500 °C for 10 h. Noticeably, about 42.8% of TOC still remained after the decolorization process was completed. Moreover, the mineralization rate become very slow after the UV-irradiation of about 100 min, indicating the formation of some long-lived by-products, which have low rate constants of reactions with hydroxyl radicals. Indeed, even an extended irradiation of over 140 min did not induce a complete conversion of the organic materials to water, carbon dioxide and other inorganic species, and about 15% of TOC still remained.

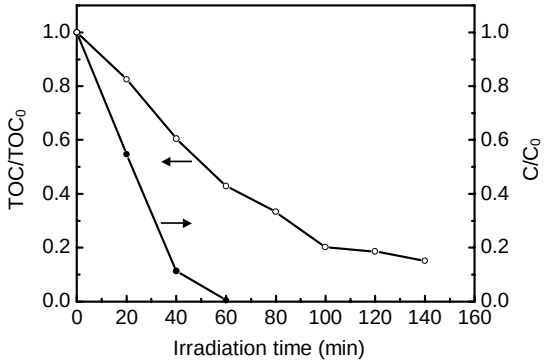

Fig. 6. TOC elimination kinetics of MO over the Z_2S_1 calcined at 500 °C for 10 h (TOC_0 and TOC are the total organic carbon concentrations of the MO suspensions before and after UV-irradiation, respectively). Z_2S_1: 2.5 g l^{-1}; MO: 20 mg l^{-1}.

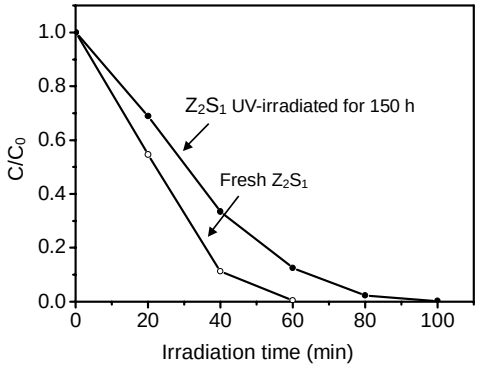

Fig. 7. Comparison for the photocatalytic activities of the Z_2S_1 calcined at 500 °C for 10 h before and after 150 h UV-irradiation.

The photo-stability of the Z_2S_1 photocatalyst calcined at 500 °C for 10 h is shown in Fig. 7. It can be seen that the photocatalytic activity became lower after the photocatalyst was UV-irradiated for 150 h. The XRD analysis indicates no changes in the phase composition of the photocatalyst after 150 h UV-irradiation (not shown). But the XRD results cannot rule out the possibility of the formations of some amorphous products such as amorphous $Zn(OH)_2$, $SnO_2{\cdot}nH_2O$, Zn and Sn with no photocatalytic activity under the UV-irradiation. It is possible that one or more of amorphous $Zn(OH)_2$, $SnO_2{\cdot}nH_2O$, Zn and Sn formed under the UV-irradiation, which led to the decrease in the photocatalytic activity. But a further study is needed on this issue.

4. Conclusion

The nanosized coupled ZnO/SnO_2 photocatalysts were prepared with the coprecipitation method followed by calcinations, and their phase compositions, mean sizes and band gap energies, as well as their photocatalytic activities, were studied with regard to their Sn contents and calcination temperatures. The photocatalytic activity of the coupled photocatalysts, evaluated by using MO photodegradation as a probe reaction, reached their maximum when the Sn content was about 33.3 mol% and calcination temperature was about 500 °C. The hetero-junctions ZnO/SnO_2 in the coupled ZnO/SnO_2 photocatalysts might be responsible for the enhancement of their photocatalytic activity. The coupled ZnO/SnO_2 photocatalyst with a Sn content of 33.3 mol% calcined at 500 °C for 10 h was found to be relatively stable and an effective photocatalyst for the degradation of methyl orange.

Acknowledgements

The authors thank Mr. Jingzhi Wei, Mr. Yu Liang and Mr. Yu Wu for their helps in this work.

References

[1] M.R. Hoffmann, S.T. Martin, W.Y. Choi, D.W. Bahnemann, Chem. Rev. 95 (1995) 69.
[2] K. Tennakone, J. Bandara, Appl. Catal. A: Gen. 208 (2001) 335.
[3] K. Vinodgopal, P.V. Kamat, Environ. Sci. Technol. 29 (1995) 841.
[4] X.Z. Li, F.B. Li, C.L. Yang, W.K. Ge, J. Photochem. Photobiol. A: Chem. 141 (2001) 209.
[5] B. Pal, M. Sharon, G. Nogami, Mater. Chem. Phys. 59 (1999) 254.
[6] X.Z. Fu, L.A. Clark, Q. Yang, M.A. Anderson, Environ. Sci. Technol. 30 (1996) 647.
[7] J. Lin, J.C. Yu, J. Photochem. Photobiol. A: Chem. 116 (1998) 63.
[8] H.P. Klug, L.E. Alexander, X-ray Diffraction Procedures for Polycrystalline and Amorphous Materials, Wiley, New York, 1974, p. 618.
[9] T. Hashemi, H.M. Al-allak, J. Illingsworth, A.W. Brinkman, J. Woods, J. Mater. Sci. Lett. 9 (1990) 776.
[10] F. Belliard, P.A. Connor, J.T.S. Irvine, Solid State Ionics 135 (2000) 163.
[11] J.H. Yu, G.M. Choi, Sens. Actuators B: Chem. 61 (1999) 59.
[12] N. Daneu, A. Recnik, S. Bernik, D. Kolar, J. Am. Ceram. Soc. 83 (2000) 3165.
[13] J.H. Yu, G.M. Choi, Sens. Actuators B: Chem. 52 (1998) 251.
[14] Y. Gao, H.B. Zhao, B.Y. Zhao, J. Mater. Sci. 35 (2000) 917.
[15] P.L. Provenzano, G.R. Jindal, J.R. Sweet, W.B. White, J. Lumin. 92 (2001) 297.
[16] A. Hagfeldt, M. Gratzel, Chem. Rev. 95 (1995) 49.
[17] Z.Y. Chen, Y. Jia, Z.D. Zhang, Y.T. Qian, J. Univ. Sci. Technol. China 17 (1987) 343 (in Chinese).
[18] W. Spence, J. Appl. Phys. 38 (1967) 3767.
[19] B.S. Kawasaki, B.K. Garside, J. Shewchun, Proc. IEEE 58 (1970) 179.
[20] F.J. Arlinghaus, J. Phys. Chem. Solids 35 (1974) 931.
[21] L.X. Cao, F.J. Spiess, A.M. Huang, S.L. Suib, T.N. Obee, S.O. Hay, J.D. Freihaut, J. Phys. Chem. B 103 (1999) 2912.
[22] K.L. Chopra, S. Major, D.K. Pandya, Thin Solid Films 102 (1983) 1.
[23] J.H. Park, P.M. Woodward, Int. J. Inorg. Mater. 2 (2000) 153.
[24] A.L. Linsebigler, G.Q. Lu, J.T. Yates Jr., Chem. Rev. 95 (1995) 735.
[25] C. Wang, X.M. Wang, J.C. Zhao, B.X. Mai, G.Y. Sheng, P.A. Peng, J.M. Fu, J. Mater. Sci. 37 (2002) 2989.
[26] C. Wang, J.C. Zhao, X.M. Wang, G.Y. Sheng, P.A. Peng, J.M. Fu, Appl. Catal. B: Environ. 39 (2002) 269.